

**Carbon Chain Formation on Metallic Arrays. X-ray
Structural Determinations of
[Ru₄(μ₄-(CCC(CO₂Me)C(CO₂Me))(η-C₅H₄R)₂(μ-CO)(CO)₈),
[Ru(CO)₂(η-C₅H₅)₂{μ-C(CO₂Me)=C(CO₂Me)C(O)}],
and [Ru(CO)₂(η-C₅H₅)₂{μ-C=C(CN)₂C=C(CN)₂}]
(R = H, Me)**

Lindsay T. Byrne, James P. Hos, George A. Koutsantonis,* Vanessa Sanford,
Brian W. Skelton, and Allan H. White

*Department of Chemistry, University of Western Australia, Nedlands,
Perth, Western Australia, Australia 6907*

Received March 2, 2001

The open, planar Ru₄C₂ compounds [Ru₄(μ₄-CC)(η-C₅H₄R)₂(μ-CO)₂(CO)₈] (R = H, Me) react with the activated electron-deficient alkyne dimethyl acetylenedicarboxylate, (CO₂Me)₂C₂ (DMAD), to afford a number of products. One of these was found to contain a metallacyclopentadiene ligand ligated at the 1- and 2-positions by Ru(η-C₅H₄R) groups, and another was a new Ru₂ compound resulting from the coupling of DMAD, C₂, and CO to produce a five-carbon chain.

Introduction

We have been interested in modeling the carbon–carbon bond-forming reactions central to the Fischer–Tropsch synthesis.^{1–15} This synthesis is typically catalyzed with transition metals and its outcome greatly influenced by the addition of so-called “promoters”. Although a tremendous amount of empirical research has provided efficient commercial catalysts, the ability to tailor gas-to-liquid conversion to meet changing needs is lacking. Our aim is to deal with the fundamental aspects of metal-mediated carbon–carbon bond forming reactions and their application to catalysis.

We have recently reported the synthesis of reactive tetranuclear ruthenium carbide complexes, [Ru₄(μ₄-CC)-

(η-C₅H₄R)₂(μ-CO)₂(CO)₈] (R = H, Me), which contain an open planar geometry and were found to be reactive, unlike the more condensed pentanuclear complexes we had previously reported.^{16,17} We are using these tetranuclear complexes to explore the reactivity of the C₂²⁻ ligand in a metal coordination environment.¹⁸

Herein we report the reaction of [Ru₄(μ₄-CC)(η-C₅H₄R)₂(μ-CO)₂(CO)₈] (R = H (**1a**), Me (**1b**)) with the alkyne dimethyl acetylenedicarboxylate (DMAD), together with the reaction of [Ru(CO)₂(η-C₅H₅)₂(μ-CC)] with DMAD and tetracyanoethylene (TCNE).

Results

Syntheses. Complexes **1**, formed in situ, were found to react readily at ambient temperatures with a slight excess of DMAD, giving three fractions (TLC) (Scheme 1). The products were separated by radial chromatography under argon. The first fraction eluted was identified as [Ru₃(CO)₁₂], retained from the in situ formation of **1**. The second fraction was isolated as a waxy orange material and tentatively assigned as [Ru₄(C₂C(CO₂Me)C(CO₂Me))(η-C₅H₄R)₂(CO)₉] (**2**; yield ca. 20%), on the basis of analytical and spectroscopic data. The final fraction (light orange) band was recrystallized from CH₂-Cl₂ and identified as [Ru₄(μ₄-(CCC(CO₂Me)C(CO₂Me))(η-C₅H₄R)₂(μ-CO)(CO)₈] (**3**; yield ca. 20%), which were both structurally characterized.

On one occasion the reaction of **1** and DMAD yielded another red-brown product, in addition to **2** and **3**, eluting after these two orange bands. This previously

* To whom correspondence should be addressed. Fax: +61-8-93807247. E-mail: gak@chem.uwa.edu.au.

(1) Gambarotta, S.; Edema, J. J. H.; Minhas, R. K. *Catal. Lett.* **1993**, *22*, 67.

(2) Das, D.; Ravichandran, G.; Chakrabarty, D. K.; Piramanayagam, S. N.; Shringi, S. N. *J. Mol. Catal.* **1994**, *86*, 221.

(3) Bukur, D. B.; Nowicki, L.; Lang, X. S. *Appl. Catal., A: Gen.* **1995**, *128*, 13.

(4) Kim, J. S.; Dai, H. L. *Catal. Today* **1995**, *23*, 17.

(5) Ming, H.; Baker, B. C. *J. Am. Chem. Soc.* **1995**, *117*, 2606.

(6) Boellaard, E.; Vanderkraan, A. M.; Geus, J. W. *Fuel Proc. Technol.* **1996**, *48*, 189.

(7) Herrmann, W. A. *Appl. Homogeneous Catal. Organomet. Compd.* **1996**, *2*, 747.

(8) Hussain, S. T. *Catal. Rev.–Sci. Eng.* **1996**, *38*, 249.

(9) Wohlers, M.; Herzog, B.; Belz, T.; Bauer, A.; Braun, T.; Ruhle, T.; Schlögl, R. *Chem. Commun.* **1996**, *7*, 1.

(10) Xu, L.; Bao, S.; O'Brien, R. J.; Raje, A.; Davis, B. H. *CHEMTECH* **1998**, *28*, 47.

(11) Guzzi, L.; Kiricsi, I. *Appl. Catal., A* **1999**, *186*, 375.

(12) Maitlis, P. M.; Quyoum, R.; Long, H. C.; Turner, M. L. *Appl. Catal., A* **1999**, *186*, 363.

(13) Van der Laan, G. P.; Beenackers, A. A. C. M. *Catal. Rev. – Sci. Eng.* **1999**, *41*, 255.

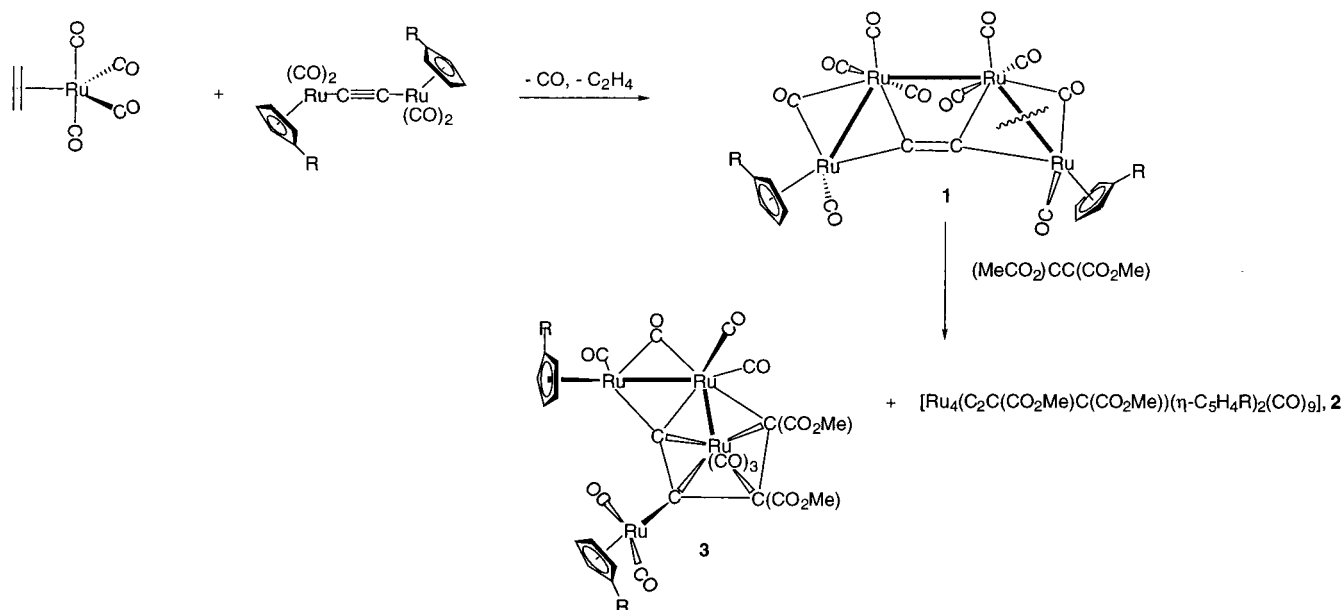
(14) Silva, R.; Schmal, M.; Frety, R.; Dalmon, J. A. *J. Chem. Soc., Chem. Commun.* **1993**, *21*, 1670.

(15) Ganzerla, R.; Lenarda, M.; Storaro, L.; Bertocello, R. *Stud. Surf. Sci. Catal.* **1998**, *119*, 131.

(16) Byrne, L. T.; Griffith, C. S.; Hos, J. P.; Koutsantonis, G. A.; Skelton, B. W.; White, A. H. *J. Organomet. Chem.* **1998**, *565*, 259.

(17) Byrne, L. T.; Hos, J. P.; Koutsantonis, G. A.; Skelton, B. W.; White, A. H. *J. Organomet. Chem.* **1999**, *592*, 95.

(18) Byrne, L. T.; Hos, J. P.; Koutsantonis, G. A.; Skelton, B. W.; White, A. H. *J. Organomet. Chem.* **2000**, *598*, 28.

Scheme 1^a

^a Legend: **a**, R = H; **b**, R = Me.

unobserved product was recrystallized (CH₂Cl₂/*n*-hexane) and identified by spectroscopic and microanalytical techniques as $[\{\text{Ru}(\text{CO})_2(\eta\text{-C}_5\text{H}_5)\}_2\{\mu\text{-CCC}(\text{CO}_2\text{Me})=\text{C}(\text{CO}_2\text{Me})\text{C}(\text{O})\}]$ (**4**). It was apparent that complex **4** probably resulted from the reaction of DMAD with unreacted $[\{\text{Ru}(\text{CO})_2(\eta\text{-C}_5\text{H}_5)\}_2(\mu\text{-CC})]$, remaining from the in situ formation of **1**. We probed this possibility with the direct reaction of $[\{\text{Ru}(\text{CO})_2(\eta\text{-C}_5\text{H}_5)\}_2(\mu\text{-CC})]$ and DMAD, which proceeded readily, recognized by a rapid change of color, giving a quantitative yield of **4** (IR, NMR). Given the facility of the reaction with DMAD, we also reacted $[\{\text{Ru}(\text{CO})_2(\eta\text{-C}_5\text{H}_5)\}_2(\mu\text{-CC})]$ with tetracyanoethylene (TCNE). The product of this reaction was very insoluble, giving a very pale yellow precipitate of $[\{\text{Ru}(\text{CO})_2(\eta\text{-C}_5\text{H}_5)\}_2\{\mu\text{-}(\text{CN})_2\text{C}=\text{CC}=\text{C}(\text{CN})_2\}]$ (**5**), which contained a $\mu\text{-trans-2,3}$ -butadienediyl ligand.

The FAB MS of complexes **2** and **3** both contain a molecular ion, corresponding to $[\text{Ru}_4(\text{C}_5\text{H}_4\text{R})_2(\text{CO})_9\text{C}_2\text{C}_2(\text{CO}_2\text{Me})_2]^+$ (R = H, Me), suggestive of their possible isomeric nature. These spectra showed extensive fragmentation, with losses of both OMe and CO groups observed. The solution IR spectra are similar. Absorbances at 1717 and 1722 cm⁻¹ are assigned to the ester carbonyl stretches and bridging M–CO bands at 1813 and 1822 cm⁻¹ for **2** and **3**, respectively.

The ¹H NMR spectra for the complexes **2a** and **3a** each show two sets of methoxy resonances at 3.77, 3.79 ppm and 3.60, 3.80 ppm. The two sets of inequivalent cyclopentadienyl protons are observed with notably broad resonances for **2a** at 5.27 and 5.37 ppm, compared to the sharp signals at 5.20 and 5.57 ppm for **3a**. The $\eta\text{-C}_5\text{H}_4\text{Me}$ analogues **2b** and **3b** show similar methoxy resonances. The two inequivalent methyl cyclopentadienyl protons are present as a broad singlet at 2.60 ppm in **2b** and as two sharp singlets at 2.12 and 2.17 ppm in **3b**. The resonances for eight CH methylcyclopentadienyl protons for each compound fall in the expected range of 4.7–5.7 ppm and are coupled in the usual fashion.

The ¹³C NMR spectra of complexes **2** and **3** show significant differences. Omitting the obvious differences between $\eta^5\text{-C}_5\text{H}_5$ and $\eta^5\text{-C}_5\text{H}_4\text{Me}$, we assign the spectra of complexes **3** as follows. Resonances for the two inequivalent acetylenic carbon nuclei (–CCO₂Me) are assigned to signals at 109.2 and 168.2 ppm with the two inequivalent ester carbonyls assigned to singlets at 145.1 and 139.4 ppm, respectively. The previous ethene-like carbides from complex **1b** have significantly different environments in **3b**, with C(1) triply bridging, assigned to 193.6 ppm, and the other doubly bridging, assigned to 174.1 ppm. The five carbonyl signals in the spectra imply some fluxional process in complex **3b**, which contains nine inequivalent CO ligands in the solid state. An intense resonance at 199.6 ppm is assigned to all three carbonyls on Ru(3) and two less intense resonances at 199.8 and 200.6 ppm to the two sets of carbonyls on Ru(4) and Ru(2), respectively. The signals on Ru(2) resonate further downfield, consistent with its more shielded environment, bound to two metal atoms. The remaining terminal carbonyl on Ru(1) is assigned to 196.0 ppm, with the bridging carbonyl assigned the outermost signal at 234.4 ppm.

The assignment of resonances found in the NMR spectra of complex **2b** is difficult without structural information. The resonance at very low field (298.5 ppm) implies a unique mode of coordination, possibly a μ_3 carbonyl, although the infrared spectrum of **2b** does not seem to confirm this hypothesis. This signal at ca. 300 ppm in the carbon spectrum of **2b** appears to be indicative of a cumulenyl carbon, possibly a vinylidene or carbyne; it is difficult to compare this with similar structures in the literature due to the lack of reported ¹³C NMR data.^{19–25} A bridging carbonyl is assigned to

(19) Bruce, M. I. *J. Cluster Sci.* **1997**, *8*, 293.

(20) Bruce, M. I. *Organomet. Chem.* **1999**, *27*, 151.

(21) Bruce, M. I. *Chem. Rev.* **1998**, *98*, 2797–2858.

(22) Bruce, M. I. *Coord. Chem. Rev.* **1997**, *166*, 91.

(23) Sappa, E. *J. Organomet. Chem.* **1999**, *573*, 139.

(24) Bruce, M. I.; Humphrey, P. A.; Miyamae, H.; Skelton, B. W.; White, A. H. *J. Organomet. Chem.* **1992**, *429*, 187.

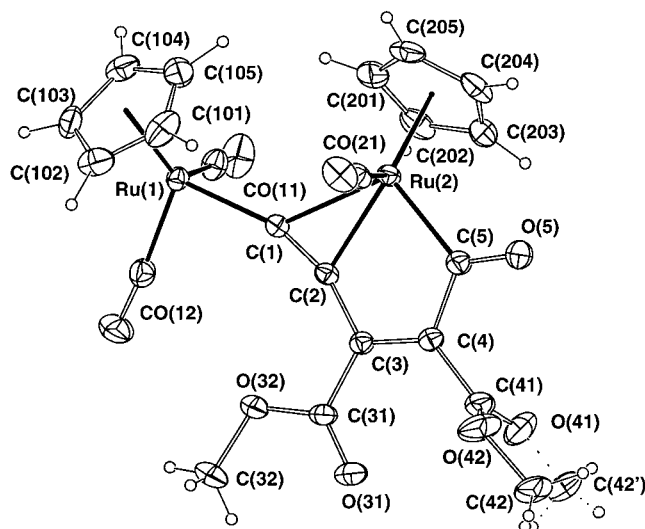


Figure 2. Molecular projection of complex **4**, almost normal to the Ru_2C_5 plane. Disorder in one of the CO_2Me groups is indicated by the dotted lines. Ellipsoids are at the 20% probability level for the non-hydrogen atoms; hydrogen atoms have arbitrary radii of 0.1 Å.

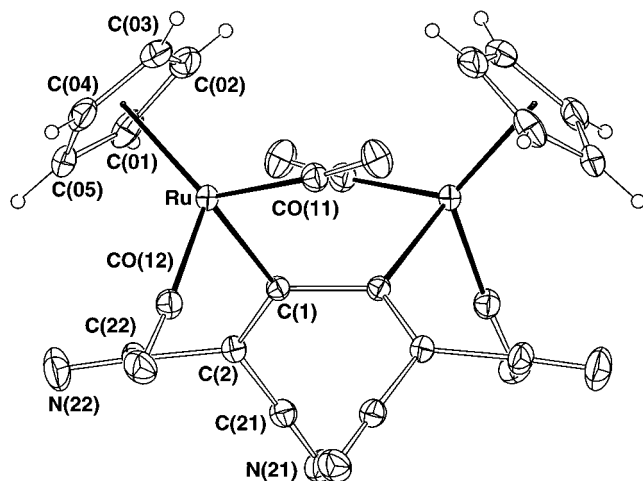


Figure 3. Molecular projection of complex **5**. Ellipsoids are at the 20% probability level for the non-hydrogen atoms; hydrogen atoms have arbitrary radii of 0.1 Å.

in all three structures **3b**, **6**, and **7** (**3b**, 2.034(3) and 2.085(3) Å; **6**, 2.06(2) and 2.07(2) Å; **7**, 2.08(2) and 2.10(2) Å) and lie in the region expected for Ru–C single bonds. The angles about C(1), C(2) and C(3), C(4) are suggestive of a significant deviation from sp^2 hybridization ($\text{Ru}(2)\text{--C}(2)\text{--C}(3) = 67.6(1)^\circ$, $\text{Ru}(3)\text{--C}(4)\text{--Ru}(2) = 79.47(9)^\circ$, compared to $\text{C}(2)\text{--C}(3)$, which has near-ideal sp^2 hybridization ($\text{Ru}(4)\text{--C}(2)\text{--C}(3) = 124.0(2)^\circ$).

The structure of the dinuclear complex **4** established that one molecule of DMAD had been incorporated into the complex which, interestingly, had coupled with the carbide unit and an additional CO molecule, giving a ruthenium-coordinated acyl ligand. The $\text{C}(1)\text{--C}(2)$ bond distance has increased marginally (ca. 0.06 Å) from the strictly CC triple bond found in the starting material, [$\{\text{Ru}(\text{CO})_2(\eta\text{-C}_5\text{H}_5)\}_2(\mu\text{-CC})$], indicating that significant triple-bond character remains. The resonance structures shown (Figure 5) indicate an alternative interpretation of the $\eta^2\text{-C}=\text{C}$ bond to Ru(2). Thus, the ligand found in **4** can be considered as an acyl $\sigma, \eta^2(3e)$ -pentadienyl (**C**)

or acyl $\sigma, \eta^2(3e)$ -enynyl (**D**) moiety, depending on the interpretation of the bond lengths and angles. The most relevant comparison here is the related acyl complex [$\text{Ru}\{\text{C}(\text{O})\text{C}(\text{Ph})=\text{C}(\text{Ph})\text{-}\eta^2\text{-C}(\text{Ph})=\text{CH}(\text{Ph})\}\{\text{P}(\text{OMe})_3\}_2(\eta\text{-C}_5\text{H}_5)$] (**8**). The ligand in this molecule is an acyl formally derived from penta-2,4-dien-1-one.

The geometry about both C(1) and C(2) in **4** is typical of “bent back” alkyne coordination with close to ideal sp^2 geometries observed at C(3) and C(4). Examination of relevant bond angles reveals an $\text{Ru}(1)\text{--C}(1)\text{--C}(2)$ angle of $160.6(2)^\circ$ with $\text{C}(1)\text{--C}(2)\text{--C}(3) = 161.4(3)^\circ$; the acyl portions of the ligands in **4** and **8** are more closely comparable. The Ru–C(O) bonds are similar (**4**, 2.088(4) Å; **8**, 2.040(12) Å) and $\text{C}(5)\text{--C}(4)$ bonds are also similar (**4**, 1.498(5) Å; **8**, 1.515(15) Å). Thus, the description of the ligand in complex **4** is that of an enyne incorporating a ruthenium-substituted η^2 -alkyne (**4'**). The $\text{C}(3)\text{--C}(4)$ bond distances in **4** and **8** are similar (**4**, 1.352(4) Å; **8**, 1.340(16) Å), with $\text{C}(1)\text{--C}(2)$ being significantly longer. The $\text{C}(5)\text{--Ru}(2)$ bond distance in **4** is unremarkable and characteristic of a metal–carbon σ -bond. The distance $\text{C}(4)\text{--C}(5)$ is long compared to $\text{C}(3)\text{--C}(4)$, ruling out any resonance along this part of the chain.

The solid-state structure of complex **5** confirmed the incorporation of TCNE into [$\{\text{Ru}(\text{CO})_2(\eta\text{-C}_5\text{H}_5)\}_2(\mu\text{-CC})$], giving a *cis*-(μ -tetracyanobutadiene-2,3-diyl)diruthenium complex. There are a number of examples of TCNE reacting with ruthenium alkynyl complexes to give related products, but only one where the reaction of ethynediyl complexes was studied. These diplatinum complexes, [$\{\text{PtCl}(\text{PMe}_3)_3\}_2\{\mu\text{-C}=\text{C}(\text{CN})_2\text{C}=\text{C}(\text{CN})_2\}$] (**9**), exhibit stereoisomerism with both *cis* and *trans* isomers with respect to the metal atoms, but complex **5** is clearly *cis*. The geometry about the ruthenium atom does not appear to be unduly affected by the electron-withdrawing ligand and is similar to that found for other $\text{Ru}(\text{CO})_2(\eta\text{-C}_5\text{H}_5)$ units. However, the tetracyanobutadienyl ligand compares well with the analogous ligand found in **9**. In both complexes **5** and **9** the metal–C bonds are single, lying well within the range for such distances. The *cis*- μ -tetracyanobutadiene-2,3-diyl ligands share many similarities, with $\text{C}(1)\text{--C}(2)$ (**5**, 1.370(2) Å; **9**, 1.36(1) Å) clearly a double bond and $\text{C}(1)\text{--C}(1')$ a single bond (**5**, 1.465(2) Å; **9**, 1.47(1) Å). The geometry about C(1) is clearly sp^2 with $\text{M}\text{--C}(1)\text{--C}(2)$, $\text{C}(2)\text{--C}(1)\text{--C}(1')$, and $\text{M}\text{--C}(1)\text{--C}(1')$ approximately 120° (**5**, $123.4(1)$, $117.5(1)$, and $119.1(1)^\circ$; **9**, $119.2(8)$, $119.4(10)$, and $118.1(7)^\circ$). The larger $\text{M}\text{--C}(1)\text{--C}(2)$ angle for **5** is most likely a result of the increased steric encumbrance of the $\text{Ru}(\text{CO})_2(\eta\text{-C}_5\text{H}_5)$ moiety.

Discussion

Reaction of 1 with DMAD (Scheme 1). The activation of carbon monoxide and its coupling to a hydrocarbon chain is of relevance to FT chemistry. There are a number of examples of this type of migratory insertion reaction in mononuclear chemistry,³⁷ but examples are less commonly found with cluster-bound hydrocarbons. Some recent examples are the reported insertion of CO into an Ru–C bond, giving the structural fragment **10**,²²

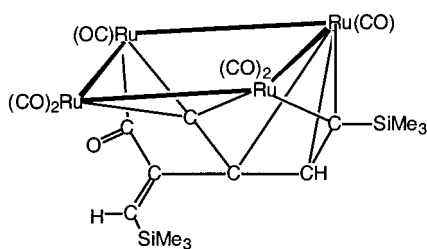
(37) Cavell, K. J. *Coord. Chem. Rev.* **1996**, *155*, 209.

Table 1. Crystal/Refinement Data for Complexes 3–5

	3a	3b	4 ^a	5
formula	C ₂₇ H ₁₆ O ₁₃ Ru ₄	C ₂₉ H ₂₀ O ₁₃ Ru ₄	C ₂₂ H ₁₆ O ₈ Ru ₂	C ₂₂ H ₁₆ N ₄ O ₈ Ru ₂
<i>M_r</i>	952.7	980.7	610.5	596.5
cryst syst	triclinic	triclinic	monoclinic	monoclinic
space group	<i>P</i> $\bar{1}$ (<i>C</i> ₁ ¹ , No. 2)	<i>P</i> $\bar{1}$ (<i>C</i> ₁ ¹ , No. 2)	<i>P</i> 2 ₁ / <i>c</i> (<i>C</i> _{2h} ⁶ , No. 14)	<i>P</i> 2 ₁ / <i>n</i> (<i>C</i> _{2h} ⁴ , No. 13)
<i>a</i> (Å)	9.786(1)	9.6402(7)	12.270(1)	8.3685(2)
<i>b</i> (Å)	11.209(2)	11.5159(9)	10.107(1)	7.8859(6)
<i>c</i> (Å)	13.945(2)	14.7985(11)	17.521(2)	16.355(1)
α (deg)	81.903(2)	80.740(1)		
β (deg)	72.796(2)	76.015(1)	95.624(2)	101.912(1)
γ (deg)	90.413(3)	89.916(1)		
<i>V</i> (Å ³)	1444.7	1572.2	2162.3	1056.1
<i>D_c</i> (g cm ⁻³)	2.19 ₀	2.07 ₁	1.87 ₅	1.87 ₆
μ (cm ⁻¹)	21.2	19.5	14.4	14.7
specimen (mm)	0.12 × 0.10 × 0.07	0.29 × 0.23 × 0.08	0.45 × 0.13 × 0.07	0.70 × 0.15 × 0.15
<i>T</i> _{min} , <i>T</i> _{max}	0.54, 0.80	0.66, 0.84	0.66, 0.85	0.72, 0.89
<i>N_t</i>	14346	18268	25129	12173
<i>N</i> (<i>R</i> _{int})	7210(0.045)	7645(0.020)	5483(0.020)	2672(0.019)
<i>N_o</i>	5491	6382	3937	2473
<i>R</i>	0.062	0.026	0.032	0.020
<i>R_w</i>	0.074	0.031	0.039	0.033
<i>n_v</i>	397	496	299	166
$\Delta\rho$ _{max} (e Å ⁻³)	3.5(1)	0.67(3)	0.94(4)	0.68(2)
<i>T</i> (K)	ca. 153	ca. 300	ca. 300	ca. 300

^a In **4**, the (carboxy-) methyl group was modeled as disordered over two sites, associated with the two oxygen atoms, implying unresolved disorder therein (etc) also; occupancies were refined to 0.57(1) and its complement.

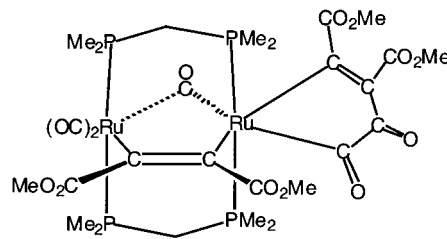
and [Ru₃(CO)₆(μ -2-CO)(μ -2-AsPh₂)(μ -2-OCC₁₂H₁₇)]³⁸ (**11**; C₁₂H₁₇ = 1,6-cyclododecadien-1-yl-3-ylidene).



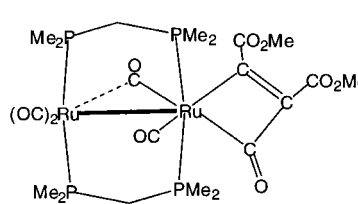
Complex 10

In considering the formation of complexes **3**, we found that there are numerous examples of metallacyclopentadienyl ligands in the literature resulting from the oligomerization of alkynes at group 8 metals.³⁹ However, there are few examples of this type of ligand where one of the ring carbons is metalated, the most recent examples being derived from the reaction of a cluster-bound allenylidene and internal alkynes, [Ru₃(CO)₉{ μ -3-C(R)C(R)C₂CPh₂}]³⁹ (**12**). It is important to note that DMAD is an activated electron-deficient alkyne and reacts readily in a wide range of organometallic systems. We expected that **1** would experience reactivity at the “long” Ru–Ru bond,¹⁸ which spans the inner two Ru atoms, but it is obvious from the product obtained that one of the Ru(CO)–Ru(η -C₅H₅) bonds is cleaved. It is this observation that suggested to us that the reaction probably proceeds initially by way of reaction at the carbide unit. While DMAD participates readily in cycloaddition reactions, a number of dipolar intermediates can be drawn which rationalize the oligomerization reactions it sometimes undergoes. Gladfelter⁴⁰ has proposed a single-electron transfer to DMAD as a possible first step in its reaction with [Ru₂(dmpm)₂(CO)₅]; one of the products, **13**, is the result of an

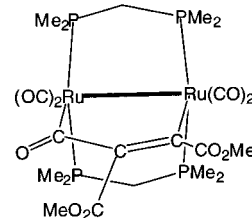
unusual double insertion of CO, the others being variants on this theme (**14**–**16**), with **16** being the ultimate thermodynamic product. Recent work⁴¹ has suggested that with the availability of vacant coordination sites, e.g. in [Ru(CH₃CN)₂(CO)(η -C₅H₅)]⁺, oligomerization of terminal and internal alkynes proceeds through well-accepted coordination and activation pathways, giving ruthenium cyclopentadienone derivatives, **17**.



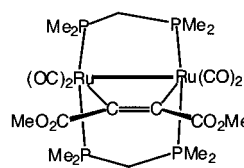
Complex 13



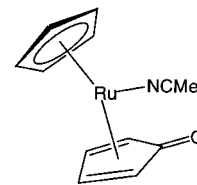
Complex 14



Complex 15



Complex 16



Complex 17

Given these numerous alternatives, it is difficult to propose a definitive mechanism, but it is clear that Ru-

(38) bin Shawkataly, O.; Puvanesvary, K.; Fun, H. K.; Sivakumar, K. *J. Organomet. Chem.* **1998**, *565*, 267.

(39) Charmant, J. P. H.; King, P. J.; Quesada-Pato, R.; Sappa, E.; Schaefer, C. *J. Chem. Soc., Dalton Trans.* **2001**, *1*, 46.

(40) Johnson, K. A.; Gladfelter, W. L. *Organometallics* **1992**, *11*, 2534.

(41) Rueba, E.; Mereiter, K.; Soldouzi, K. M.; Gemel, C.; Schmid, R.; Kirchner, K.; Bustelo, E.; Puerta, M. C.; Valerga, P. *Organometallics* **2000**, *19*, 5384.

Table 2. Selected Geometries for 3a and 3b^a

Ruthenium Environments ^{b,c}							
(i) Ru(2)							
atom	<i>r</i>	C(21)		C(22)		C(1)	
C(12)	2.103(9), 2.089(3)	89.1(4), 87.6(1)		101.6(4), 99.4(1)		93.3(4), 94.3(1)	
C(21)	1.93(1), 1.960(4)			92.1(5), 94.1(2)		163.3(4), 162.8(1)	
C(22)	1.853(9), 1.856(3)					103.6(4), 102.5(1)	
C(1)	2.04(1), 2.034(3)						
C(4)	2.085(9), 2.085(3)					75.6(4), 75.7(1)	
(ii) Ru(3)							
atom	<i>r</i>	C(32)		C(33)		C(1)	
C(31)	1.92(1), 1.916(3)	96.4(4), 97.2(1)		94.9(4), 94.9(2)		100.9(4), 101.9(1)	
C(32)	1.92(1), 1.919(3)			90.7(5), 90.4(1)		158.8(3), 158.2(1)	
C(33)	1.90(1), 1.916(4)					99.8(4), 98.2(1)	
C(1)	2.315(8), 2.298(3)					35.4(3), 35.60(9)	
C(2)	2.318(8), 2.327(2)					61.7(3), 61.95(9)	
C(3)	2.220(8), 2.226(2)					37.1(4), 37.2(1)	
C(4)	2.215(9), 2.229(3)						
(iii) Ru(1) ^d							
atom	<i>r</i>	C(12)		C(1)		C(100)	
C(11)	1.849(9), 1.858(3)	84.8(4), 85.9(1)		89.5(4), 90.5(1)		127. ₆ , 126. ₆	
C(12)	2.11(1), 2.094(4)			93.9(4), 94.2(1)		120. ₆ , 120. ₉	
C(1)	2.016(9), 2.034(3)					128. ₃ , 127. ₆	
C(100)	1.91 ₂ , 1.91 ₃						
(iv) Ru(4) ^e							
atom	<i>r</i>	C(42)		C(2)		C(400)	
C(41)	1.88(1), 1.881(3)	91.2(4), 90.1(1)		91.2(4), 91.3(1)		126. ₆ , 127. ₂	
C(42)	1.896(9), 1.873(3)			91.8(4), 91.3(1)		124. ₀ , 125. ₂	
C(2)	2.13(1), 2.125(3)					122. ₂ , 121. ₄	
C(400)	1.89 ₅ , 1.91 ₃						
(b) Ligand Geometries							
Distances (Å)							
C(1)–C(2)	1.41(1), 1.414(4)		C(12)–O(12)		1.15(1), 1.174(4)		
C(2)–C(3)	1.45(1), 1.457(4)		C(3)–C(311)		1.51(1), 1.513(4)		
C(3)–C(4)	1.43(1), 1.436(4)		C(4)–C(411)		1.49(1), 1.494(4)		
Angles							
O(12)–C(12)–Ru(1)	133.1(9), 134.9(3)		C(1)–C(2)–C(3)		109.2(8), 108.4(3)		
O(12)–C(12)–Ru(2)	145.7(9), 143.3(3)		C(2)–C(3)–C(4)		115.6(8), 115.8(2)		
Ru(1)–C(12)–Ru(2)	81.1(3), 81.8(1)		C(2)–C(3)–C(311)		122.7(9), 123.1(3)		
Ru(1)–C(1)–Ru(2)	84.9(3), 84.6(1)		C(4)–C(3)–C(311)		121.3(9), 120.7(3)		
Ru(1)–C(1)–C(2)	150.6(8), 150.3(2)		Ru(3)–C(4)–Ru(2)		79.0(3), 79.47(9)		
Ru(2)–C(1)–C(2)	122.8(7), 123.2(2)		C(3)–C(4)–Ru(2)		116.5(7), 116.3(2)		
Ru(4)–C(2)–C(1)	126.5(7), 127.4(2)		C(3)–C(4)–C(411)		117.1(8), 116.6(2)		
Ru(4)–C(2)–C(3)	124.1(6), 124.0(2)		Ru(2)–C(4)–C(411)		126.0(7), 126.7(2)		

^a C(π 00) is the centroid of Cp ring C(π 01–5). ^b *r* is the ruthenium–ligand atom distance (Å), with the first value associated with **3a** and the second with **3b**; the other entries in each matrix comprise the angles (deg) subtended by the associated atoms at the head of each row and column. ^c Ru(2)–Ru(1,3) lengths are 2.737(1), 2.7387(4) Å and 2.738(1), 2.7598(4) Å. Ru(1)–Ru(2)–Ru(3) angles are 90.94(3), 89.96(1)°. ^d Ru(1)–C(10*n*) ranges: 2.21(1)–2.297(9), 2.195(4)–2.313(3) Å. ^e Ru(4)–C(40*n*) ranges: 2.227(9)–2.259(9), 2.236(3)–2.304(3) Å.

(3)–Ru(4) (Scheme 2) is cleaved. This could be promoted by alkyne coordination or a result of the direct reaction of the C₂²⁻ ligand with the electron-poor alkyne. Concomitant with this, cleavage coordination and/or coupling of the DMAD through presumably polar intermediates followed or preceded by CO expulsion and cleavage of Ru(2)–Ru(3) leads to complexes **3**. It should be noted that **1** is rigid in solution, at least on the NMR time scale, and proposing intermediates such as **1'** (Scheme 2) would appear fruitless. Obviously the formation of these compounds is complex, as we have yet to account for the formation of **2**.

Reaction of [Ru(CO)₂(η -C₅H₅)₂(μ -CC)] with DMAD and TCNE. The observation of complex **4** in the preceding reaction was the stimulus for the further investigation of the reactivity of [Ru(CO)₂(η -C₅H₅)₂-

(μ -CC)] with activated substrates. In this case the carbide unit reacted directly with DMAD and TCNE. As mentioned previously, DMAD is thought to react via radical mechanisms,⁴⁰ while the cycloaddition of TCNE to transition-metal alkynyl complexes via transient radicals is well-known.^{42–51} The alkynyl dianion is electron rich and obviously reacts readily with DMAD,

(42) Onitsuka, K.; Ose, N.; Ozawa, F.; Takahashi, S. *J. Organomet. Chem.* **1999**, *578*, 169.

(43) Stokes, H. L.; Ni, L. M.; Belot, J. A.; Welker, M. E. *J. Organomet. Chem.* **1995**, *487*, 95.

(44) Su, S. R. Thesis, Ohio State University, Columbus, OH, 1971.

(45) Su, S. R.; Wojcicki, A. *Inorg. Chim. Acta* **1974**, *8*, 55.

(46) Yamamoto, Y.; Satoh, R.; Tanase, T. *J. Chem. Soc., Dalton Trans.* **1995**, 307.

(47) Kergoat, R.; Kubicki, M. M.; Gomes de Lima, L. C.; Scordia, H.; Guerschais, J. E.; L'Haridon, P. *J. Organomet. Chem.* **1989**, *367*, 143.

Table 3. Selected Geometries for 4^a

Distances (Å)			
Ru(1)–C(100)	1.89 ₈	Ru(2)–C(200)	1.93 ₇
Ru(1)–C(10 <i>n</i>)	2.222(4)–	Ru(2)–C(20 <i>n</i>)	2.228(4)–
(range)	2.246(4)	(range)	2.311(5)
Ru(1)–C(11)	1.879(4)	Ru(2)–C(21)	1.838(4)
Ru(1)–C(12)	1.870(4)	Ru(2)–C(1)	2.300(3)
Ru(1)–C(1)	2.029(3)	Ru(2)–C(2)	2.155(3)
C(1)–C(2)	1.250(4)	Ru(2)–C(5)	2.088(4)
C(2)–C(3)	1.421(4)	C(3)–C(31)	1.479(5)
C(3)–C(4)	1.352(4)	C(5)–O(5)	1.216(4)
C(4)–C(5)	1.498(5)		
Angles (deg)			
C(100)–Ru(1)–C(1)	125. ₀	C(200)–Ru(2)–C(1)	119. ₀
C(100)–Ru(1)–C(11)	129. ₀	C(200)–Ru(2)–C(2)	134. ₃
C(100)–Ru(1)–C(12)	124. ₈	C(200)–Ru(2)–C(21)	128. ₆
C(1)–Ru(1)–C(11)	87.1(2)	C(200)–Ru(2)–C(5)	118. ₀
C(1)–Ru(1)–C(12)	88.5(1)	C(1)–Ru(2)–C(2)	32.4(1)
C(11)–Ru(1)–C(12)	90.0(2)	C(1)–Ru(2)–C(21)	90.6(1)
Ru(1)–C(1)–C(2)	160.6(2)	C(1)–Ru(2)–C(5)	107.9(1)
Ru(1)–C(1)–Ru(2)	131.9(1)	C(2)–Ru(2)–C(21)	93.7(1)
Ru(2)–C(1)–C(2)	67.4(2)	C(2)–Ru(2)–C(5)	76.0(1)
Ru(2)–C(2)–C(1)	80.2(2)	C(21)–Ru(2)–C(5)	86.0(2)
Ru(2)–C(2)–C(3)	116.6(2)	C(2)–C(3)–C(31)	122.6(3)
C(1)–C(2)–C(3)	161.4(3)	C(4)–C(3)–C(31)	121.3(3)
C(2)–C(3)–C(4)	115.9(3)	C(4)–C(5)–O(5)	119.4(3)
C(3)–C(4)–C(5)	115.1(3)	Ru(2)–C(5)–O(5)	124.3(3)
Ru(2)–C(5)–C(4)	116.3(2)		

^a C(*n*00) is the centroid of Cp ring C(*n*01–5).

Table 4. Selected Geometries for 5^a

Distances (Å)			
Ru–C(100)	1.89 ₅	C(1)–C(1')	1.465(2)
Ru–C(0 <i>n</i>) (range)	2.233(2)–2.249(2)	C(2)–C(21)	1.438(2)
Ru–C(11)	1.889(2)	C(2)–C(22)	1.439(3)
Ru–C(12)	1.893(2)	C(21)–N(21)	1.139(3)
Ru–C(1)	2.099(1)	C(22)–N(22)	1.136(3)
C(1)–C(2)	1.370(2)		
Angles (deg)			
C(100)–Ru–C(1)	126. ₉	Ru–C(1)–C(1')	119.1(1)
C(100)–Ru–C(11)	124. ₃	C(2)–C(1)–C(1')	117.5(1)
C(100)–Ru–C(12)	122. ₁	C(1)–C(2)–C(21)	122.9(2)
C(1)–Ru–C(11)	91.73(8)	C(1)–C(2)–C(22)	122.8(2)
C(1)–Ru–C(12)	86.33(7)	C(2)–C(21)–N(21)	178.3(2)
C(11)–Ru–C(12)	95.17(8)	C(2)–C(22)–N(22)	177.6(2)
Ru–C(1)–C(2)	123.4(1)		

^a C(100) is the centroid of the Cp rings; primed atoms are related by the intramolecular 2-axis.

but it is impossible to say whether a radical mechanism is operating in this case. However, formally one can speculate (Scheme 3) that the first step involves nucleophilic attack of the dianion at DMAD to form **B** followed by attack at a coordinated carbonyl. It is unlikely that DMAD coordinates a ruthenium, given that our recent work suggests that $[\{\text{Ru}(\text{CO})_2(\eta\text{-C}_5\text{H}_5)\}_2(\mu\text{-CC})]$ is rather inert to substitution. It is noteworthy that acyl pentadienyl complexes similar to **4** are implicated in the formation of ruthenium cyclopentadienone complexes.⁴¹

While this paper was in preparation, the reaction of group 10 ethynediyl complexes, $[\{\text{MCl}(\text{PR}_3)_2\}(\mu\text{-C}\equiv\text{C})]$, with TCNE was reported,⁴² these reactions yielding both the *cis*- and *trans*-(μ -tetracyanobutadiene-2,3-diyl)di-

platinum complexes **9**. The mechanism operating in this type of reaction is now well understood (Scheme 4). The first step is a [2 + 2] cycloaddition of TCNE to the triple bond of $[\{\text{Ru}(\text{CO})_2(\eta\text{-C}_5\text{H}_5)\}_2(\mu\text{-CC})]$ to give an intermediate cyclobutene-1,2-diyl complex, which then ring-opens to give complex **5**. It was interesting to find that only the *cis* isomer of **5** was obtained, given that the steric requirements of a $\text{Ru}(\text{CO})_2(\eta\text{-C}_5\text{H}_5)$ unit should outweigh those of $\text{MCl}(\text{PR}_3)_2$ (M = Pt, Pd) in **9**, where the *trans* isomer appeared to be the thermodynamic product. Heating a DMSO solution of complex **5** for a prolonged period (weeks) resulted in the formation of several uncharacterized products with ca. 50% of the sample unchanged. There was no conclusive evidence for the formation of a *trans* isomer.

Summary

We have described the reaction of activated substrates such as the electron-poor DMAD and TCNE with ruthenium complexes containing the alkynyl dianion, C_2^{2-} . In all reactions we have observed the formation of chains containing four, five, or six carbon atoms. In one instance we have also observed the activation of CO and isolated complexes that shed considerable light on well-trodden alkyne oligomerization reactions. It is also clear that the complexes presented here clearly implicate the C_2^{2-} unit in the formation of carbon chains, which could have implications for the mechanism of the Fischer–Tropsch reaction. Maitlis¹² has provided convincing evidence for the implication of vinyl intermediates in FT chemistry which finds support in the CC bond-forming reactions of the permetalated ethene ligand in **1**.

Experimental Section

General Comments. Manipulation of oxygen- and moisture-sensitive compounds was performed under an atmosphere of high-purity argon using standard Schlenk techniques or in a drybox (Miller Howe).

Infrared spectra were recorded using a Bio-Rad FTS 45 or 40 FTIR spectrometer. ¹H and ¹³C NMR spectra were acquired using Varian Gemini 200 and Bruker ARX 500 spectrometers. ³¹P NMR spectra were acquired using a Bruker ARX 500 spectrometer. ¹H and ¹³C NMR spectra were referenced with respect to incompletely deuterated solvent signals.

Mass spectra were obtained on a VG AutoSpec spectrometer employing a fast atom bombardment (FAB) ionization source in all samples, unless otherwise specified.

Elemental analyses were performed by The Research School of Chemistry Microanalytical Unit, Australian National University, Australian Capital Territory, Australia.

Tetrahydrofuran was dried over sodium metal and distilled from potassium benzophenone ketyl under an atmosphere of argon. Hexanes and toluene were dried over sodium metal and distilled under an atmosphere of argon. Distilled solvents were stored over sodium or potassium mirrors until use.

$[\text{Ru}_4(\mu_4\text{-CC})(\eta\text{-C}_5\text{H}_4\text{R})_2(\mu\text{-CO})_2(\text{CO})_8]$ (R = H (**1a**), Me (**1b**))¹⁸ and $[\{\text{Ru}(\text{CO})_2(\eta\text{-C}_5\text{H}_5)\}_2(\mu\text{-CC})]$ ⁵² were prepared according to previously reported routes.

Structure Determinations. Full spheres of area-detector diffraction data were measured using a Bruker AXS CCD

(52) Koutsantonis, G. A.; Selegue, J. P. *J. Am. Chem. Soc.* **1991**, *113*, 2316.

(53) Hall, S. R.; King, G. S. D.; Stewart, J. M. *The XTAL 3.4 User's Manual*; University of Western Australia: Lamb, Perth, 1995.

(48) Bruce, M. I.; Hambley, T. W.; Snow, M. R.; Swincer, A. G. *Organometallics* **1985**, *4*, 494.

(49) Bruce, M. I.; Hambley, T. W.; Snow, M. R.; Swincer, A. G. *Organometallics* **1985**, *4*, 501.

(50) Bruce, M. I.; Hambley, T. W.; Rodgers, J. R.; Snow, M. R.; Swincer, A. G. *J. Organomet. Chem.* **1982**, *226*, C1.

(51) Bruce, M. I.; Hambley, T. W.; Snow, M. R.; Swincer, A. G. *J. Organomet. Chem.* **1982**, *235*, 105.

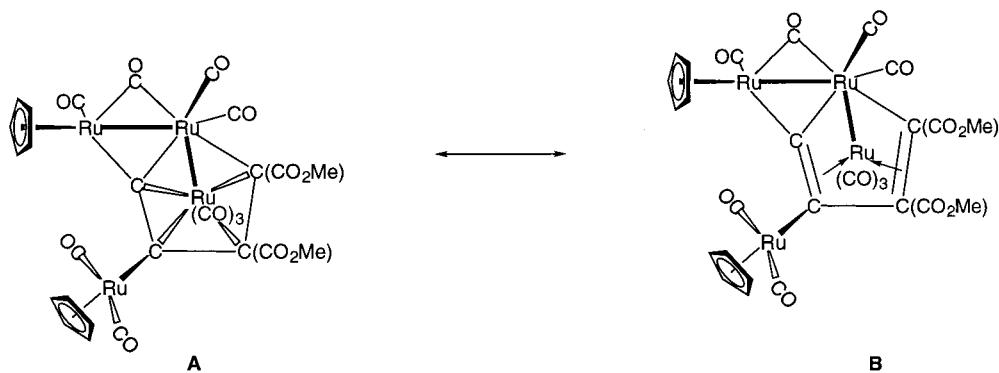


Figure 4. Alternative representations of complex **3a**.

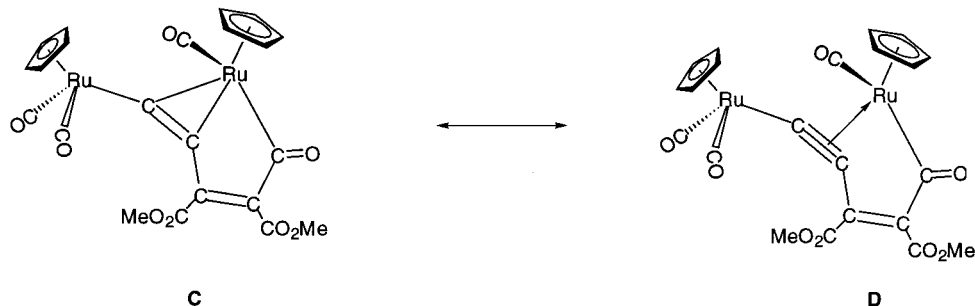
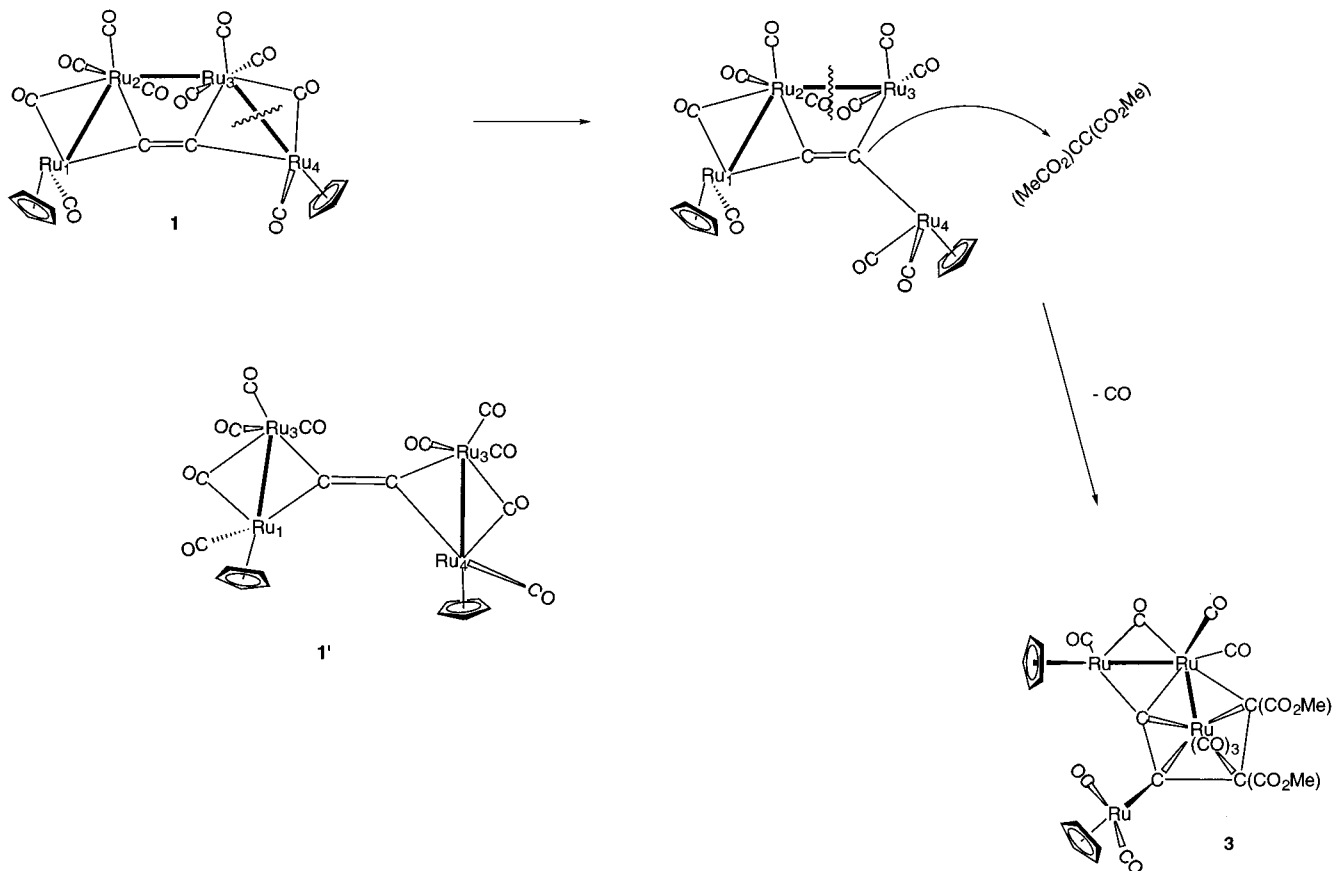


Figure 5. Alternative representations of complex **4**.

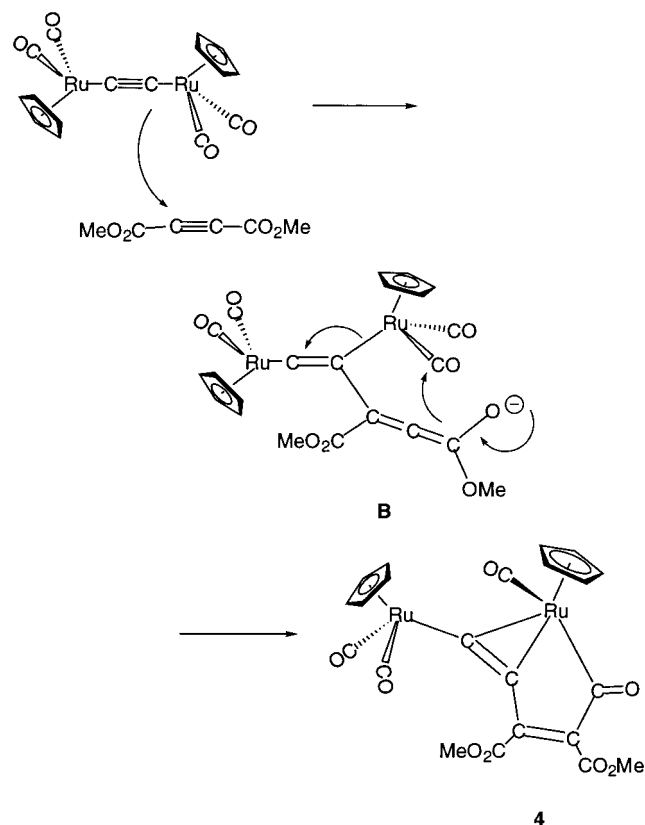
Scheme 2



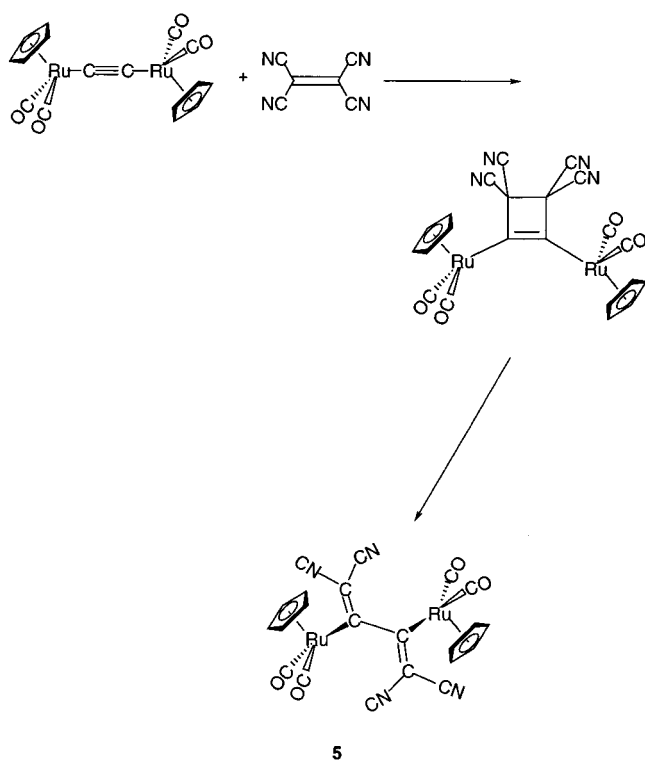
instrument fitted with monochromatic Mo $K\alpha$ radiation source ($\lambda = 0.71073 \text{ \AA}$) within the limit $2\theta_{\max} = 58^\circ$. $N_{(\text{total})}$ reflections were acquired, reducing to N_{unique} (R_{int} quoted) incorporating "empirical" absorption corrections (proprietary software), N_0 of these with $F > 4\sigma(F)$ being used in the full matrix least squares refinements. Anisotropic thermal parameters were

refined for the non-hydrogen atoms, (x, y, z, U_{iso})_H being refined for **3b** and **5** and included constrained at estimated values for **3a** and **4**. Conventional residuals on $|F|$, R , R_w (statistical weights) are quoted at convergence. Neutral atom complex scattering factors were employed, computation using the Xtal 3.4 program system.⁵³ Atomic coordinates are deposited with

Scheme 3



Scheme 4



the Cambridge Crystallographic Data Base (deposition numbers 157509–157512).

Syntheses. $[\text{Ru}_4(\mu_4\text{-}(\text{CC})\text{C}(\text{CO}_2\text{Me})\text{C}(\text{CO}_2\text{Me}))(\eta\text{-C}_5\text{H}_5)_2(\mu\text{-CO})(\text{CO})_8]$ (**3a**). DMAD (20 μL , 0.162 mmol) and **1a** (100 mg, 0.105 mmol) were stirred for ca. 14 h in THF at ambient temperature. The solvent was removed in vacuo, and the residue was applied to a radial chromatography plate which

was developed with acetone/*n*-hexane. The first red-orange band was eluted with ca. 10% acetone/hexanes and collected, and the volatiles were removed, giving a waxy red solid (**2a**; 20 mg, 19%), formulated as $\text{Ru}_4(\text{C}_5\text{H}_5)_2\text{C}_2\text{C}_2(\text{CO}_2\text{Me})_2(\text{CO})_9$. IR ($\nu(\text{CO})$): 2098 w, 2076 m, 2048 vs, 2004 s, 1976 m, 1818 w br, 1710 w br cm^{-1} . $^1\text{H NMR}$ (δ ; CDCl_3): 3.77 (s, 3H, CO_2Me), 3.79 (s, 3H, CO_2Me), 5.27 (s br, 5H, C_5H_5), 5.36 (s br, 5H, C_5H_5). $^{13}\text{C}\{^1\text{H}\}$ NMR (δ ; CDCl_3): 52.0 (s, CO_2Me), 52.6 (s, CO_2Me), 84.1 (s, CC), 92.9, 93.3 (s, $2 \times \text{C}_5\text{H}_5$), 114.7 (s, $\text{C-CO}_2\text{Me}$), 146.0 (s (br), $2 \times \text{CO}_2\text{Me}$), 166.6 (s, $\text{C-CO}_2\text{Me}$), 172.1 (s, $\mu_3\text{-CC}$), 198.4 (s, $7 \times \text{CO}$), 237.4 (s, $\mu\text{-CO}$), 295.8 (s, Ru-C). FAB MS (NOBA/ CH_2Cl_2): m/z 954 ($[\text{M}]^+$, 100%), 923 ($[\text{M} - \text{OMe}]^+$, 65%), 898, 870, 841, 815, 785 ($[\text{M} - \text{Ome} - n\text{CO}]^+$, $n = 1-5$, 40%, 45%, 45%, 55%, 40%). The next light orange band was collected, the volatiles were removed, and the residue was recrystallized ($\text{CHCl}_3/\text{hexanes}$) to give bright orange crystals of **3a**· CHCl_3 (16 mg, 14%). Anal. Calcd for $\text{C}_{28}\text{H}_{17}\text{Cl}_3\text{O}_{13}\text{Ru}_4$: C, 31.36; H, 1.60. Found: C, 31.72; H, 1.53. IR ($\nu(\text{CO})$): 2116 w, 2077 m, 2051 vs, 2003 s, 1976 m, 1818 w br, 1713 w br cm^{-1} . $^1\text{H NMR}$ (δ ; CDCl_3): 3.60 (s, 3H, CO_2Me), 3.78 (s, 3H, CO_2Me), 5.20 (s, 5H, C_5H_5), 5.57 (s, 5H, C_5H_5). $^{13}\text{C}\{^1\text{H}\}$ NMR (δ ; CDCl_3): 52.2 (s, CO_2Me), 52.7 (s, CO_2Me), 88.9 (s, C_5H_5), 89.0 (s, C_5H_5), 109.2 (s, $\text{Ru-C-CO}_2\text{Me}$), 139.3 (s, CO_2Me), 139.4 (s, CO_2Me), 168.2 (s, $\mu\text{-C-CO}_2\text{Me}$), 174.1 (s, $\mu\text{-CC}$) 193.6 (s, $\mu_3\text{-CC}$), 196.0 (s, CO), 199.6 (s, $3 \times \text{CO}$), 199.8 (s, $2 \times \text{CO}$), 200.6 (s, $2 \times \text{CO}$), 234.2 (s, $\mu\text{-CO}$). FAB MS (NOBA/ CH_2Cl_2): m/z 954 ($[\text{M}]^+$, 100%), 926, 898, 870, 842, 814, 786 ($[\text{M} - n\text{CO}]^+$, $n = 1-6$, 33%, 35%, 22%, 20%, 30%, 20%), 586 ($[\text{M} - \text{CpRu}(\text{CO})_2 - 2\text{OMe}]^+$, 35%).

$[\text{Ru}_4(\mu_4\text{-}(\text{CC})\text{C}(\text{CO}_2\text{Me})\text{C}(\text{CO}_2\text{Me}))(\eta\text{-C}_5\text{H}_4\text{Me})_2(\mu\text{-CO})(\text{CO})_8]$ (**3b**). In a manner similar to that for **3a**, DMAD (20 μL , 0.162 mmol) was reacted with **1b** (97 mg, 112 μmol) in THF to yield first a yellow band, eluted with hexane, and identified as $\text{Ru}_3(\text{CO})_{12}$ (23 mg), presumably from the in situ formation of **1b**. A red band as a waxy red solid (**2b**; 22 mg, 20%) was formulated as $\text{Ru}_4(\text{C}_5\text{H}_4\text{Me})_2\text{C}_2\text{C}_2(\text{CO}_2\text{Me})_2(\text{CO})_9$. IR ($\nu(\text{CO})$): 2098 w, 2076 m, 2046 vs, 2003 s, 1971 m, 1813 w br, 1717 w br cm^{-1} . $^1\text{H NMR}$ (δ ; CDCl_3): 2.06 (s, 6H), 3.75 (s, 3H, CO_2Me), 3.80 (s, 3H, CO_2Me), 4.70–5.40 (m, 8H, $2 \times \text{C}_5\text{H}_4\text{Me}$). $^{13}\text{C}\{^1\text{H}\}$ NMR (δ ; CDCl_3): 12.4 (s, $2 \times 2 \times \text{C}_5\text{H}_4\text{Me}$), 52.0 (s, CO_2Me), 52.6 (s, CO_2Me), 83.3 (s, CC), 88.1, 89.0, 89.5, 91.6, 93.2, 95.5, 96.8 (s, $2 \times \text{C}_5\text{H}_4\text{Me}$), 114.9 (s, $\text{C-CO}_2\text{Me}$), 145.1 (s (br), $2 \times \text{CO}_2\text{Me}$), 166.8 (s, $\text{C-CO}_2\text{Me}$), 172.3 (s, $\mu_3\text{-CC}$), 198.7 (s, $7 \times \text{CO}$), 241.6 (s, $\mu\text{-CO}$), 298.5 (s, Ru-C). FAB MS (NOBA/ CH_2Cl_2): m/z 982 ($[\text{M}]^+$, 65%), 952 ($[\text{M} - \text{OMe}]^+$, 100%), 927, 898, 869, 843, 814, 785, 756, 729 ($[\text{M} - \text{Ome} - n\text{CO}]^+$, $n = 1-8$, 50%, 65%, 70%, 45%, 60%, 35%, 35%, 30%).

The next light orange band was eluted with 30% acetone/hexanes, giving bright orange crystals of **3b** (24 mg, 22%) after recrystallization from $\text{CH}_2\text{Cl}_2/\text{hexanes}$. Anal. Calcd for $\text{C}_{29}\text{H}_{20}\text{O}_{13}\text{Ru}_4$: C, 35.50; H, 2.05. Found: C, 35.56; H, 2.08. IR (CH_2Cl_2 ; $\nu(\text{CO})$): 2112 w, 2064 m, 2039 vs, 2000 m, 1983 s, 1822 m br, 1722 m br cm^{-1} . $^1\text{H NMR}$ (δ ; CDCl_3): 2.12 (s, 3H, $\text{C}_5\text{H}_4\text{Me}$), 2.17 (s, 3H, $\text{C}_5\text{H}_4\text{Me}$), 3.60 (s, 3H, CO_2Me), 3.79 (s, 3H, CO_2Me), 4.91 (m, 2H, $\text{C}_5\text{H}_4\text{Me}$), 4.95 (m, 1H, $\text{C}_5\text{H}_4\text{Me}$), 5.91 (m, 1H, $\text{C}_5\text{H}_4\text{Me}$), 5.25 (m, 1H, $\text{C}_5\text{H}_4\text{Me}$), 5.30 (m, 1H, $\text{C}_5\text{H}_4\text{Me}$), 5.39 (m, 1H, $\text{C}_5\text{H}_4\text{Me}$), 5.47 (m, 1H, $\text{C}_5\text{H}_4\text{Me}$). $^{13}\text{C}\{^1\text{H}\}$ NMR (δ ; CDCl_3): 13.0 (s, $\text{C}_5\text{H}_4\text{Me}$), 13.6 (s, $\text{C}_5\text{H}_4\text{Me}$), 51.9 (s, CO_2Me), 52.4 (s, CO_2Me), 84.2 (s, $2 \times \text{C}_5\text{H}_4\text{Me}$), 85.1 (s, $2 \times \text{C}_5\text{H}_4\text{Me}$), 85.6 (s, $2 \times \text{C}_5\text{H}_4\text{Me}$), 86.6 (s, $2 \times \text{C}_5\text{H}_4\text{Me}$), 93.4 (s, $\text{C}_5\text{H}_4\text{Me}$), 93.6 (s, $\text{C}_5\text{H}_4\text{Me}$), 109.2 (s, $\text{Ru-C-CO}_2\text{Me}$), 139.3 (s, CO_2Me), 139.4 (s, CO_2Me), 168.2 (s, $\mu\text{-C-CO}_2\text{Me}$), 174.1 (s, $\mu\text{-CC}$) 193.6 (s, $\mu_3\text{-CC}$), 196.0 (s, CO), 199.6 (s, $3 \times \text{CO}$), 199.8 (s, $2 \times \text{CO}$), 200.6 (s, $2 \times \text{CO}$), 234.4 (s, $\mu\text{-CO}$). FABMS (NOBA/ CH_2Cl_2): m/z 982 ($[\text{M}]^+$, 100%), 954, 926, 898 ($[\text{M} - n\text{CO}]^+$, $n = 1-3$, 30%, 35%, 20%), 867 ($[\text{M} - 3\text{CO} - \text{OMe}]^+$, 18%), 843, 815 ($[\text{M} - n\text{CO}]^+$, $n = 5-6$, 12%, 16%).

$[\text{Ru}_2\{\mu\text{-CCC}(\text{CO}_2\text{Me})\text{C}(\text{CO}_2\text{Me})\text{C}(\text{O})\}(\eta\text{-C}_5\text{H}_5)_2(\text{CO})_4]$ (**4**). DMAD (5 μL , 45 μmol) was added to $[\{\text{Ru}(\text{CO})_2(\eta\text{-C}_5\text{H}_5)\}_2(\mu\text{-CC})]$ (10 mg, 40 μmol) in THF, with stirring. The addition was accompanied by an immediate color change from light brown

to dark brown-red. The solution was filtered through a plug of alumina and recrystallized (CH₂Cl₂/*n*-hexane) as dark brown crystals of **4** (12 mg, 95%). Anal. Calcd for C₂₂H₁₆O₈Ru₂: C, 43.27; H, 2.64. Found: C, 42.75; H, 2.39. IR (CH₂Cl₂; ν(CO)): 2052 s, 2000 vs, 1945 m, 1885 w, 1729 m cm⁻¹. ¹H NMR (δ; CD₂Cl₂): 3.76 (s, 3H, CO₂Me), 3.87 (s, 3H, CO₂Me), 5.18 (s, 5H, C₅H₅), 5.56 (s, 5H, C₅H₅). ¹³C{¹H} NMR (δ; CD₂Cl₂): 52.3 (s, CO₂Me), 53.0 (s, CO₂Me), 89.5 (s, C₅H₅), 91.3 (s, C₅H₅), 96.8 (s, C=C), 98.7 (s, μ-C=C), 145.4 (s, CCO₂Me), 158.6 (s, CCO₂-Me), 163.4 (s, CO₂Me), 165.3 (s, CO₂Me), 197.0 (s, CO), 197.0 (s, CO), 200.2 (s, CO), 240.0 (s, Ru-C(O)-C). FABMS (NOBA/CH₂Cl₂): *m/z* 612 ([M]⁺, 100%), 583, 555 ([M - *n*CO]⁺, *n* = 1-2, 25%, 45%), 523 ([M - 2CO - OMe]⁺, 5%).

[{Ru(CO)₂(η-C₅H₅)₂{μ-(CN)₂C=CC=C(CN)₂}] (**5**). TCNE (27.3 mg, 0.213 mmol) was added to [{Ru(CO)₂(η-C₅H₅)₂(μ-CC)] (100 mg, 0.213 mmol) in THF (10 mL), with stirring. The solution was stirred for 16 h, giving a pale yellow precipitate of **5** (85 mg, 67%). Anal. Calcd for C₂₂H₁₆N₄O₄Ru₂: C, 44.28; H, 1.69; N, 9.39. Found: C, 44.90; H, 1.72; N, 9.57. IR (Nujol):

ν(CO) 2051 vs, 2003 vs; ν(CN) 2215 s, 2211 s; ν(CC) 1489 m cm⁻¹. ¹H NMR (δ; *d*₆-DMSO): 5.81 (s, 5H, C₅H₅). ¹³C{¹H} CP/MAS NMR (δ) 91.1 (s, C₅H₅).

Acknowledgment. We thank the Australian Research Council and the Special Research Centre for Materials and Minerals Processing, UWA, for supporting this work. J.P.H. is the holder of an Minerals Institute of Western Australia Scholarship. We thank Dr. Allan McKinley and his group for use of a high-vacuum line.

Supporting Information Available: Tables of hydrogen and non-hydrogen positional and isotropic displacement parameters, atomic anisotropic displacement parameters, and bond distances and angles, as well as figures giving additional views for complexes **3**–**5**. This material is available free of charge via the Internet at <http://pubs.acs.org>.

OM0101745